

# Routes towards Anderson localization of Bose-Einstein condensates in disordered optical lattices

T. Schulte<sup>1</sup>, S. Drenkelforth<sup>1</sup>, J. Kuse<sup>1</sup>, W. Ertmer<sup>1</sup>, J. Arit<sup>1</sup>, K. Sacha<sup>2</sup>, J. Zakrzewski<sup>2</sup>, and M. Lewenstein<sup>3,4</sup>;

<sup>1</sup> Institut für Quantenoptik, Universität Hannover, Welfengarten 1, D-30167 Hannover, Germany

<sup>2</sup> Instytut Fizyki Mariana Smoluchowskiego, Uniwersytet Jagielloński, PL-30-059 Kraków, Poland

<sup>3</sup> Institut für Theoretische Physik, Universität Hannover, D-30167 Hannover, Germany and

<sup>4</sup> ICFO - Institut de Ciències Fòniques, 08034 Barcelona, Spain

We investigate, both experimentally and theoretically, possible routes towards Anderson localization of Bose-Einstein condensates in disordered potentials. The dependence of this quantum interference effect on the nonlinear interactions and the shape of the disorder potential is investigated. Experiments with an optical lattice and a superimposed disordered potential reveal the lack of Anderson localization. A theoretical analysis shows that this absence is due to the large length scale of the disorder potential as well as its screening by the nonlinear interactions. Further analysis shows that incommensurable superlattices should allow for the observation of the cross-over from the nonlinear screening regime to the Anderson localized case within realistic experimental parameters.

Disordered systems have played a central role in condensed matter physics in the last 50 years. Recently, it was proposed that ultracold atomic gases may serve as a laboratory for disordered quantum systems [1, 2] and allow for the experimental investigation of various open problems in that field [3]. Some of these problems concern strongly correlated systems [4], the realization of Bose [5, 12] or Fermi glasses [6], quantum spin glasses [7] and quantum percolation [8]. This letter addresses one of the most important issues, namely the interplay of Anderson localization (AL) [9] and repulsive interactions [10]. This interplay may lead to the creation of delocalized phases both for fermions [11] and bosons [12]. The possible occurrence of AL has also been investigated theoretically for weakly interacting Bose-Einstein condensates (BEC) [13], and in this case it was shown that even moderate nonlinear interaction counteracts the localization.

Several methods have been proposed to produce a disordered, or quasi-disordered potential for trapped atomic gases. They include the use of speckle radiation [14], incommensurable optical lattices [15], impurity atoms in the sample [16] and the disorder that appears close to the surface of atom chips [17]. Recently, first experiments searching for effects of disorder in the dynamics of weakly interacting BECs were realized [18].

In this letter we shed new light on the interplay between disorder and interactions by studying trapped BECs under the influence of a disordered potential and a one dimensional (1D) optical lattice. The 1D lattice creates a periodic potential and the randomness of the disordered potential leads to Anderson localization for noninteracting particles [1]. We study how the presence of interactions affects this scenario.

Our experiments were performed with <sup>87</sup>Rb Bose-Einstein condensates in an elongated magnetic trap (MT) with axial and radial frequencies of  $\nu_z = 2.14$  Hz and  $\nu_r = 2.200$  Hz, respectively. Further details of our experimental apparatus were described previously [19].

The number of condensed atoms  $N$  was varied between  $1.5 \cdot 10^4$  and  $8 \cdot 10^4$ . The optical lattice (OL) was provided by a retroreflected laser beam at  $\lambda = 825$  nm superimposed on the axial direction of the magnetic trap. The depth of the optical lattice was typically set to  $6.5 E_r$ , where the recoil energy is given by  $E_r = \hbar^2 k^2 / 2m$ . For this configuration the peak chemical potential varied between  $0.25 E_r$  and  $0.5 E_r$ . The disorder potential (DP) was produced by projecting the image of a randomly structured chrome substrate onto the atoms giving rise to a spatially varying dipole potential along the axial direction of the cloud. Due to the resolution of the imaging system the minimal structure size of the DP was limited to  $7 \mu\text{m}$ . We define the depth of the disorder potential as twice the standard deviation of the dipole potential, analogously to [18]. The combined potential allowed for the first realization of an ultracold disordered lattice gas.

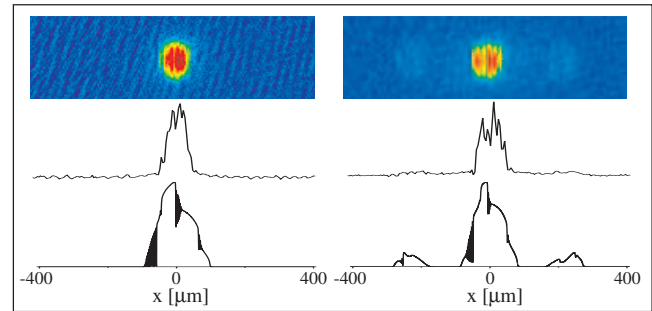


FIG. 1: Typical absorption images of a BEC with  $N = 7 \cdot 10^4$  released from the combined MT plus DP (left column) and MT plus OL plus DP (right column). The second row shows the radially summed density of the images and the third row shows a 1D simulation of both cases. The lattice depth was  $6.5 E_r$  and the disorder potential had a depth of  $0.2 E_r$ .

After the production of the BEC in the MT, we performed the following experimental sequence: We first ramped up the OL potential over 60 ms, then the DP was ramped up over another 60 ms, followed by a hold

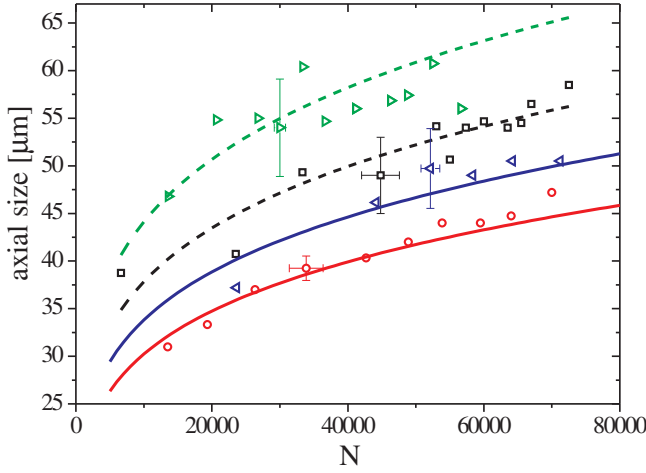


FIG. 2: Size of the central peak after 20 ms of ballistic expansion versus the atom number. The clouds were released from the following potentials MT (red), MT plus DP (black), MT plus OL (blue), MT plus DP plus OL (green). The lines correspond to a theoretical prediction (see text). The lattice depth was  $6.5 E_r$  and the disorder potential had a depth of  $0.1 E_r$ .

time of 20 ms. Finally all potentials were switched off and the atomic density distribution was measured after 20 ms of ballistic expansion using absorption imaging. Alternatively we performed the same experiment without the OL.

Figure 1 shows typical absorption images for the case of DP only and for the case of combined DP and OL. The obtained density distributions show two characteristic features. On one hand they display pronounced fringes and on the other hand the axial size of the central peak is modified with respect to the case without DP. We extract the axial size of the peak by fitting the density with a parabolic distribution. The resulting sizes are shown as a function of the atom number in Fig. 2.

Both features can be attributed to the distribution of the atoms into the wells of the disorder potential. This can lead to a slight fragmentation of the BEC and causes strong fringes in the resulting absorption images. Note that these results are in good qualitative agreement with a numerical simulation based on a 1D Gross-Pitaevskii equation (GPE) as shown in Fig. 1. The additional axial confinement due to the DP also leads to an increase of the axial size after expansion shown in Fig. 2. The red and blue curves show a theoretical prediction based on the TF approximation. For the black and green lines the same functional dependence was fitted to the experimental data. This revealed an increase in axial size by 25% and 28% respectively. We have used a 3D numerical simulation to confirm that this increase is consistent with the modification of the chemical potential, introduced by the DP. Note, that the change in size depends strongly on the exact realization of the disorder. Despite these

effects of the DP, the computed ground states reveal the absence of exponentially localized states (see the theoretical analysis given below) and we therefore conclude that the observed localization in the absorption images is not caused by quantum interference effects in the disorder potential, i.e. it does not represent Anderson localization.

In order to understand the experimental results, we consider an effective one-dimensional (1D) model. The BEC spreads over more than a hundred wells of the OL, each of the wells containing several hundreds of atoms. In this situation and for depths of the OL and DP studied here the mean-field Gross-Pitaevskii equation (GPE) description is appropriate [20]. In oscillator units corresponding to the trap frequency the GPE reads

$$i\partial_t \psi = -\frac{\partial_x^2}{2} + \frac{x^2}{2} + V_0 \cos^2(kx) + V_{\text{dis}}(x) + g|\psi|^2; \quad (1)$$

where  $V_0$  is the depth of the OL while the DP is represented by  $V_{\text{dis}}(x)$ . The coupling constant  $g$  is chosen such that the Thomas-Fermi (TF) radius equals the axial radius of the 3D atomic cloud in the experiment (for the case of  $N = 7 \cdot 10^5$  presented in Fig. 1 we obtain  $g = 1500$ ). In all further cases we have chosen  $V_0 = 6.5 E_r$ .

The disorder potential in the experiments and in the model changes on a scale much larger than the lattice spacing and the condensate healing length,  $\lambda = \lambda_c = 8 \text{ na}$ , where  $n$  is the condensate density and  $a$  the atomic scattering length. This suggests the applicability of the so-called effective mass analysis [21]. We determine the ground state solution of the stationary GPE in the form  $\psi_0(x) = \sqrt{N} f(x) u_0(x)$ , where  $u_0(x)$  is the Bloch function corresponding to the ground state of the OL potential,  $f(x)$  is an envelope function and  $N$  is a constant chosen such that  $\psi_0$  is normalized to unity. This substitution leads to an effective GPE where the optical lattice potential is eliminated but the mass of a "particle" and the interaction strength become modified. For the experimental parameters the effective mass (in oscillator units) is  $m^* = 2.56$  and the renormalized interaction strength for  $N = 7 \cdot 10^5$  is  $g = 2498$ .

Due to the large value of  $g$  we may use the TF approximation and obtain the envelope function in the form

$$|\psi(x)|^2 = \frac{x^2 + 2 V_{\text{dis}}(x)}{g}; \quad (2)$$

where  $\psi$  is determined from the condition  $\int_{-\infty}^{\infty} |\psi(x)|^2 dx = 1$ . The squared overlap of the obtained  $\psi_0$  with the exact ground state of the GPE is 0.999 which implies that the effect of the lattice potential is reduced to a modification of the coupling constant in Eqn. 2 for the TF profile of the combined MT plus DP. Thus, similarly to the experiments performed in the absence of an OL [18] we

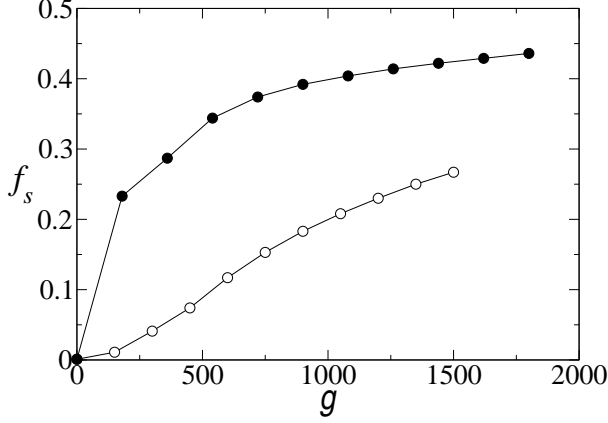


FIG. 3: Super uid fraction as a function of the coupling constant  $g$  obtained from a 1D GPE simulation for a pseudorandom potential created by two additional optical lattices at 960 nm and 1060 nm with depths of  $0.2 E_F$ . Full symbols correspond to a trap frequency of  $214$  Hz and open symbols to a trap frequency of  $24$  Hz.

observe a fragmentation of the BEC induced by the DP but this fragmentation does not correspond to Anderson localization which is caused by interference.

To enter the Anderson regime, the above analysis indicates that it is necessary to introduce a disorder that changes on a length scale comparable to the lattice spacing. Since the resolution of the imaging system responsible for the production of the DP is limited by diffraction effects this poses considerable experimental difficulties. Alternatively one may use a pseudorandom potential obtained with the help of two, or even more additional optical lattices, with incommensurable frequencies. However, even the realization of such a fine scale disorder is not necessarily sufficient for the observation of Anderson localization. Indeed, for a solution  $\psi_0$  of the stationary GPE the nonlinear term  $g|\psi_0(x)|^2$  may be treated as an additional potential. When the atoms accumulate in the wells of the random potential, the nonlinear term in the GPE effectively smoothes the potential modulations [13]. For typical experimental parameters the term  $g|\psi_0(x)|^2$  dominates over  $V_{\text{dis}}(x)$  and consequently the randomness necessary for localization is lost (for the slowly varying DP as well as a possible pseudorandom disorder).

This picture is confirmed by analyzing the dependence of the super uid fraction on the coupling constant  $g$  shown in Fig. 3. To calculate the super uid fraction we have numerically solved the 1D GPE in a box with periodic boundary conditions in the presence of an OL and a pseudorandom potential created by two additional optical lattices at 960 nm and 1060 nm with depths of  $0.2 E_F$ . The size of the box was chosen to match the size of the atomic cloud in the harmonic potential. The super uid

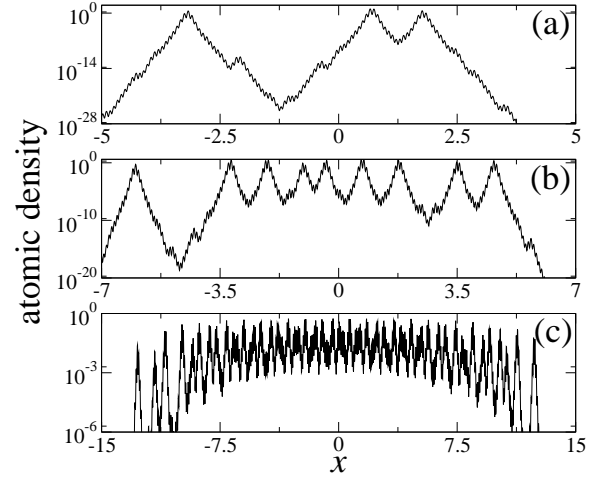


FIG. 4: Ground states of the GPE (note the varying logarithmic scales) for a condensate in the combined potential of harmonic trap, optical lattice and pseudorandom potential. The depth of the optical lattice is  $6.5 E_F$  while the depths of the additional lattices that form the pseudorandom potential are  $0.2 E_F$ . The coupling constants  $g$  for the panels are: 0.5 (a), 8 (b), 256 (c). The results are given in the oscillator units corresponding to a frequency of  $24$  Hz.

fraction is defined as  $f_s = 2[E_0(v) - E_0(0)]/Nv^2$  where  $E_0(v)$  is the ground state energy when a velocity field  $v$  is imposed on the system (i.e. we compute the ground state solution in the form  $\psi_0(x) \exp(ivx)$  where  $\psi_0(x)$  fulfills periodic boundary conditions) [22]. The super uid fraction remains large for typical experimental parameters, indicating the absence of Anderson localization.

To overcome the screening of the disorder potential the interaction within the atomic sample has to be reduced. This can be achieved by reducing the number of atoms, lowering the trap frequencies or tuning the scattering length via Feshbach resonances. Within our 1D model we have performed calculations for a trap frequency of  $24$  Hz and a pseudorandom potential equivalent to the one used for Fig. 3. For  $g = 0$  one obtains Anderson localization of the ground state wavefunction which is characterized by an exponential localization  $|\psi_0(x)|^2 \sim \exp(-|x - x_0|/l)$ , with the localization length  $l = 0.027$ . For such a non-interacting system, there might exist several localized single particle states with an energy close to the ground state. For finite observation times, condensation could occur into several of these low energy states, and several "small" condensates with different condensate wavefunctions could coexist. Figure 4 suggests that the condensate wave function becomes a combination of these localized states due to nonlinear interactions.

Increasing  $g$  causes the ground state to contain a larger number of localization centers. However, the localization length in these cases hardly deviates from the non-

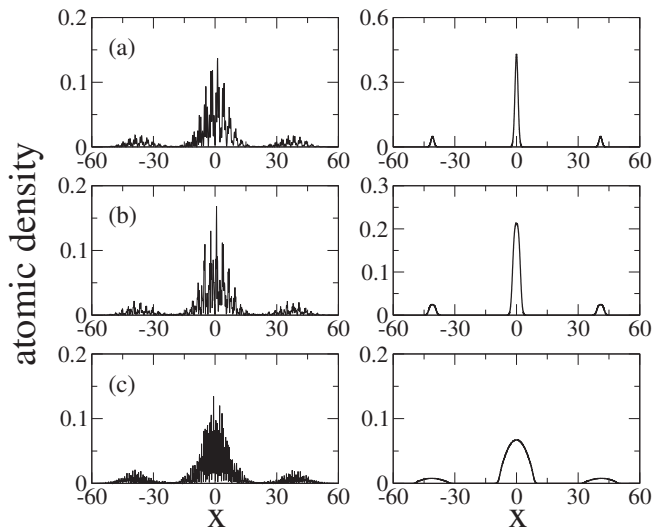


FIG. 5: Atomic density after 20 ms of ballistic expansion for a condensate prepared initially in the states shown in Fig. 4 (left column) and without DP (right column). The results are given in oscillator units corresponding to a frequency of 2 4 Hz.

interacting case. When  $g$  is of the order of 500 one can no longer distinguish individual localized states and the clear signature of Anderson localization vanishes. This is consistent with the appearance of a significant superfluid fraction in Fig. 3. The results shown in Fig. 4c for  $g = 256$  correspond to axial and radial frequencies of 2 4 Hz and 2 40 Hz, respectively and  $N = 10^4$ . In this case the simulation shows characteristic features of Anderson localization while these parameters are within experimental reach. The scenario of a cross-over from the Anderson to the screening regime, presented here, is one of the most important results of our analysis.

Our theoretical investigation also shows that the detection of the onset of Anderson localization using a measurement of the density distribution after ballistic expansion might be difficult. We have calculated the atomic density profiles after 20 ms of ballistic expansion corresponding to the parameters of Fig. 4. Despite a striking difference in the ground state wavefunction, the width of the envelope of the zero-momentum peak, which is related to the localization length  $l$ , does not vary significantly as shown in Fig. 5. In addition Fig. 5c shows that the expansion is dominated by the interaction for experimentally accessible values of  $g$  within our 1D model. Future experiments on the detection of localization may rather rely on a measurement of the superfluid fraction (see [23]) in an accelerated optical lattice.

In conclusion, we have presented a detailed analysis of Anderson localization for slowly varying potentials and in pseudorandom potentials in the presence of interactions. We have shown the absence of localization in the experimental case and explained this effect using an eff-

fective mass approach. For a truly random potential a suppression of Anderson localization due to the screening by nonlinear interactions was found. An analysis for small interactions and a pseudorandom potential reveals the characteristic features of Anderson localization. The transition from the Anderson localized to the screened delocalized regime may be detected via an analysis of the superfluid fraction. This work paves the way towards the observation of Anderson localization in an experimentally accessible regime.

We thank L. Santos, L. Sanchez-Palencia and G.V. Shlyapnikov for fruitful discussions. We acknowledge support from the Deutsche Forschungsgemeinschaft (SFB 407, SPP 1116, GK 282, 436 POL), the ESP Programme QUDEDIS, the Polish government Scientific funds PBZ-MIN-008/P03/2003 (K.S.) and LP03B08328 (2005-08) (J.Z.).

---

[\*] Also at Institutio Catalana de Recerca i Estudis Avançats.

- [1] B. Damski et al., Phys. Rev. Lett. 91, 080403 (2003).
- [2] R. Roth and K. Burnett, J. Opt. B 5, S50 (2003).
- [3] A. Sanpera et al., Phys. Rev. Lett. 93, 040401 (2004).
- [4] A. Auerbach, Interacting Electrons and Quantum magnetism, (Springer, New York, 1994).
- [5] M. P. A. Fisher, P. B. Weichman, G. Grynstein, and D. S. Fisher, Phys. Rev. B 40, 546 (1989).
- [6] R. Freedman and J. A. Hertz, Phys. Rev. B 15, 2384 (1977); Y. Imry, Europhys. Lett. 30, 405 (1995).
- [7] S. Sachdev, Quantum Phase Transitions, (Cambridge University Press, Cambridge, 1999).
- [8] Y. Shapir, A. Aharony, and A. B. Harris, Phys. Rev. Lett. 49, 486 (1982); T. Odagaki and K. C. Chang, Phys. Rev. B 30, 1612 (1984).
- [9] P. W. Anderson, Phys. Rev. 109, 5 (1958).
- [10] Y. Nagaoka and H. Fukuyama (Eds.), Anderson Localization, Springer Series in Solid State Sciences 39, (Springer, Heidelberg, 1982); T. Ando and H. Fukuyama (Eds.), Anderson Localization, Springer Proceedings in Physics 28, (Springer, Heidelberg, 1988); P. A. Lee and R. V. Ramakrishnan, Disordered electronic systems, Rev. Mod. Phys. 57, 2 (1985).
- [11] E. G. Ambetti-Cesare, D. Weinmann, R. A. Jalabert, and Ph. Bune, Europhys. Lett. 60, 120 (2002); G. Benenti, X. Waintal, and J.-L. Pichard, Phys. Rev. Lett. 83, 1826 (1999);
- [12] R. T. Scalettar, G. G. Batrouni, and G. T. Zimanyi, Phys. Rev. Lett. 66, 3144 (1991).
- [13] K. G. Singh and D. S. Rokhsar, Phys. Rev. B 49, 9013 (1994); K. O. Rasmussen, D. Cai, A. R. Bishop, and N. Grnbech-Jensen, Europhys. Lett. 47, 421 (1999); D. K. K. Lee and J. M. F. Gunn, J. Phys. C 2, 7753 (1990).
- [14] J. C. Dainty, Laser Speckle and Related phenomena, (Springer, Berlin, 1975); P. Horak, J.-Y. Courtois, and G. Grynberg, Phys. Rev. A 58, 3953 (2000).
- [15] R. B. Diener et al., Phys. Rev. A 64, 033416 (2001).
- [16] U. Gavish, and Y. Castin, cond-mat/0412671.
- [17] for a review see R. Folman et al., Adv. At. Molec. Opt.

- Phys. 48, 263 (2002); for theory see C. Henkel, P. Krüger, R. Folman, and J. Schmiedmayer, Appl. Phys. B 76, 173 (2003); D.-W. Wang, M. D. Lukin, and E. Demler, Virt. J. of Nan. Sci. Tech., 1st March (2004).
- [18] J.E. Lye et al., cond-mat/0412167; D. Clement et al., Aspect, cond-mat/0506638; C. Fort et al., cond-mat/0507144.
- [19] L. Cacciapuoti et al., Phys. Rev. A 68, 053612 (2003).
- [20] Using the Bogoliubov-de Gennes approach we have selectively checked that the depletion of the condensate is negligible for our parameters, and the GPE is therefore well justified.
- [21] M. J. Steel, and W. Zhang, arXiv:cond-mat/9810284; H. Pu et al., Phys. Rev. A 67, 043605 (2003).
- [22] E. H. Lieb, R. Seiringer, and J. Yngvason, Phys. Rev. B 66, 134529 (2002).
- [23] R. Roth and K. Burnett, Phys. Rev. A 67, 031602(R) (2003).